Development of a Small 50W Class Stirling Engine

UnChol Ri [A*], GumChol Ri [B], ChangIl Ri [A] , YongHuan Kim [A], SongJin Ri [A]

[A] *Department of renewable Energy Science, Ham Hung University of Hydraulics and Power, Ham Hung, Democratic People's Republic of Korea*
[B] *Faculty of Architecture Engineering, Ham Hung Construction University, Ham Hung, Democratic People's Republic of Korea*

[*] **Corresponding author: UnChol Ri: riunchol@163.com**

ARTICLE INFO

Keywords:
Stirling Engine
Heat Exchanger
Mechanical Loss
Engine Design

ABSTRACT

In order to develop a compact and low cost Stirling engine, a gamma type Stirling engine with simple moving-tube-type heat exchangers and a rhombic mechanism was developed. Its target shaft power is 50 W at engine speed of 4000 rpm and mean pressure of 0.8 MPa using helium as working gas. This paper describes the outline of the engine design and the performance test. The test was done without load, using air in atmospheric condition. Also, a mechanical loss measurement was done in highly pressurized condition, in which the engine was driven by a motor compulsory. Then, methods to get higher performance were considered based on the comparison of experimental and calculated results. The results indicate that a higher performance heat exchanger and decreasing of mechanical loss are needed for the attainment of the target performance.

1. INTRODUCTION

Global environment protection has come to be more and more important recently, and demand for engines with high efficiency and low pollution is increasing. Stirling engines have a potential solution to the above problems. Because of they have excellent characteristics which are high thermal efficiency, multi-fuel capability and low pollution. There are several types of Stirling cycle machine. They are being researched and developed actively all over the world. Especially the Stirling refrigerators are used practically in several fields. Low temperature differential Stirling engines are expected as power sources using solar or geothermal energy. A prototype engine that is shown in this paper is one of high temperature differential Stirling engines. As typical developments of high temperature differential Stirling engines, several high performance engines for air conditioners were developed in Moonlight project on 1982 in Japan [1]. Then, it was clarified that the Stirling engine has high efficiency and low pollution characteristics. However, the Stirling engine has not reached practical use enough, because it has several problems;i.e., a high production cost, limited endurance of no-lubricated seal devices, and heavy weight. The main purpose of this study is to develop a compact and lightweight Stirling engine with low production cost. Also, it is aimed to find a suitable type of heat exchangers and a piston drive mechanism for the compact Stirling engine. And it can predict the effects of working gas and the engine speed correspond to the maximum shaft power. On the other hand, in order to reduce the size of the engine, it is necessary that the engine be operated at higher engine speed. From a result of the simple prediction method, the engine speed at the maximum shaft power increases with the reduction of swept volume of a power piston. Figure 1 shows one of the calculated results of the relationship between mean pressure, Pm, the maximum shaft power, L_S, and engine speed, N. As the calculation conditions, swept volume of a power piston, V_E, was set to 9.9 cm3, expansion space gas temperature, T_E, was set to 600° C, and compression space gas temperature, T_C, was set to 40° C. This figure shows that shaft power of 50 W is obtained at engine speed of 4000 rpm using helium as working gas.

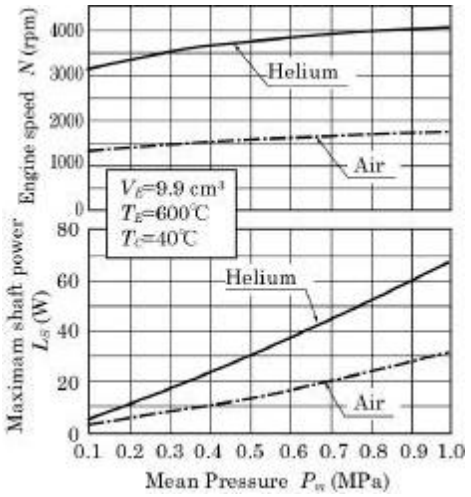

Fig. 1 Calculated result of the simple prediction method

Table 1

Target performance and specifications

Index	Value
Bore x Stroke	ϕ36×10 mm
Phase angle	90.2 deg
Working gas	Helium / Air
Target shaft power	50 W
Target efficiency	15 %
Heating method	Nichrome wire / Combustion gas
Cooling method	Water cooling
(Rated operation) Rated engine speed	4000 rpm (Helium)
(Rated operation) Mean pressure	0.8 MPa
(Rated operation) Expansion space temp	600 ℃
(Rated operation) Comp ression space temp.	40 ℃
Design (Allowable) Maximum pressure	1.1 MPa

Table 1 lists target performance and main specifications of the prototype engine. Their values were determined based on discussion of heat exchangers and a piston drive mechanism with the calculated results of the above method. Cylinder bore, piston stroke and target power were determined to be 36 mm, 10 mm and 50 W/4000 rpm, respectively. In the case of a compact engine, high efficiency is not expected, because the rate of heat conduction loss increases relatively with the reduction of the engine size. Target thermal efficiency is 15 %. This value is much lower than that of high performance Stirling engines mentioned previously. Allowable pressure in the engine was determined to be 1.1MPa with consideration of using piping parts in markets. Allowable heater wall temperature was determined based on strength and thickness of heater wall material. In this case, stainless steel (SUS304) was used as the material, and a heater was designed considering allowable heater wall temperature of 650~800°C.

2.2 BASIC STRUCTURE

A basic structure of the prototype engine was based on that of a 100 W class Stirling engine formerly developed by the author and others [3], [4]. Figure 2 shows a schematic view of the prototype engine. It was a gamma type, in which a displacer and a power piston were located in a line. A regenerator was located in the displacer. These configurations contribute to make the engine smaller. In order to get a smaller size and low production cost, a simple moving-tube-type heat exchanger was adopted as shown in Fig. 3. In the case of a moving tube type heat exchanger of the above 100W class Stirling engine, there were 10 - 24 heating tubes to get large heating surface area. However, the tubes cause high production cost. Also, high assembling accuracy is required to avoid the collision of the inner and outer tubes. From the above considerations, in the case of the prototype engine, only a couple of inner-outer tube was located in the central axis of the displacer. The inner tube of heater and the inner and outer tube of cooler were easily assembled.

Therefore, it is considered that this type of heat exchanger obtains pretty lower production cost than that of the above 100 W class Stirling engine and previous multi-tube type heat exchangers. In addition, the new type heat exchanger needs little welding. As a piston drive mechanism, it was considered to adopt a cross-head mechanism, a Scotch-yoke mechanism and other link mechanisms. Finally, a Rhombic mechanism [5] was adopted, because it gives an excellent momentum balance.

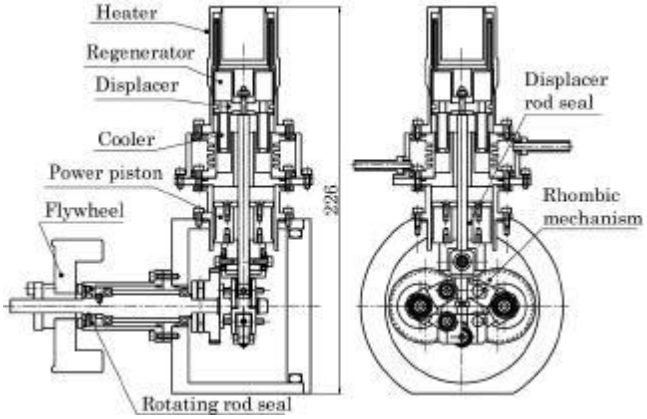

Fig. 2 Schematic view of the prototype engine

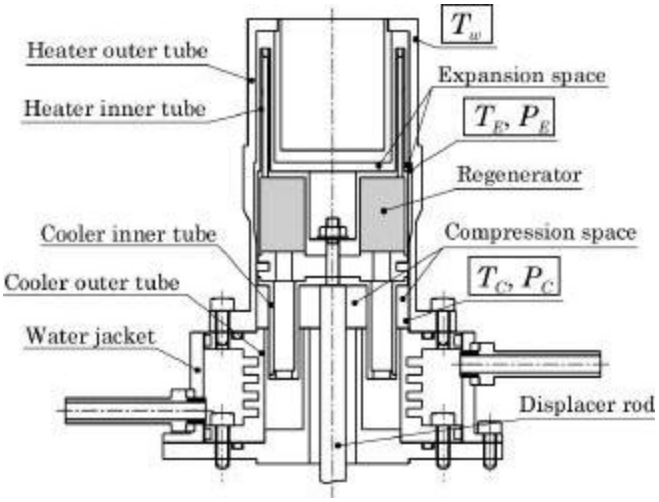

Fig. 3 Heat exchanger of the prototype engine

2.3 COMPONENTS DESIGN

(1) Heater

A heater of the prototype engine was designed using the following simple method. Heater input, *Qh*, was derived from Eqs. (1) and (2).

$$Q_h = L_E + Q_r + Q_{cd} \quad (1)$$

$$Q_h = hs(T_w - T_E) \quad (2)$$

Here, L_E is expansion power calculated from Schmidt theory [6], Q_r is reheat loss in a regenerator, Q_{cd} is heat conduction loss at a cylinder, h is heat transfer coefficient in a tube, s is heating surface area, T_E is expansion space gas temperature. Heater wall temperature, T_w, was gotten by solving simultaneous equations for Q_h in Eqs. (1) and (2). Gas flow speed needed in this calculation was based on mean piston speed of a displacer. General design method for a multi tube type heat exchanger mentioned previously was also applied to this engine, using hydraulic diameter of annular space of a moving tube-type heat exchanger.

Figure 4 shows one of the calculated results of the relationship between mean pressure, P_m, and heater wall temperature, *Tw*. Here, C_L is clearance between an inner tube and an outer tube. This figure shows that the heater wall temperature, *Tw*, of 660°C is needed to get expansion space gas temperature, T_E, of 600°C, at C_L=0.5 mm, and

Pm=0.8 MPa. Also, heat transfer performance became higher with decreasing of clearance, C_L. In order to avoid a collision between the inner and outer tube, it is necessary that the clearance, C_L, is determined with a consideration of assembling accuracy of a piston drive mechanism. Two types of heater were manufactured for the prototype engine. Their clearances were C_L=0.5 mm and C_L=1.0 mm, respectively. The collision of the tubes occurred in case of the heater of C_L=0.5 mm, thus the heater of C_L=1.0 mm was used at following experiments.

(2) Cooler

In the case of design for a cooler, both the heat transfers of gas and cooling water were taken into account in the calculation. As a result, it was confirmed that compression space gas temperature could not be kept to setting value of 40°C easily, because the heating surface area of the cooler shown in Figs. 2 and 3 was not large enough. In order to get sufficiently rejected heat, large amount of cooling water is required. Supplying sufficient water is required.

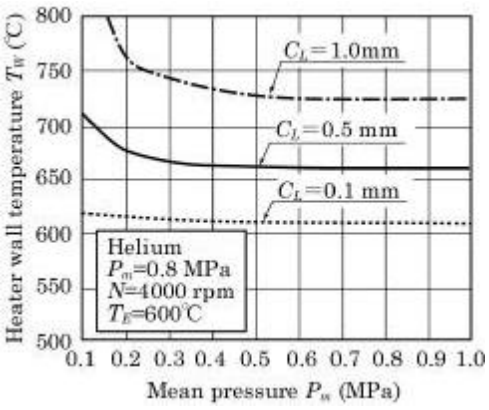

Fig. 4 Calculated result as a function of mean pressure and heater wall temperature

Supplying sufficient water was possible in the experiment, though it might not be practical.

(3) Regenerator

The shape of a displacer and its assembling method affect a size of a regenerator. After the discussion on this size optimization, outer diameter of the regenerator was determined to be 34 mm, inner diameter was determined to be 13 mm, and height was determined to be 17.5 mm. In the following experiments, wire gauze made of brass (#100, diameter of 0.1 mm, 70 sheets) was used as a regenerator matrix.

Shapes and locations of manifolds to a heater and cooler tube affect flow of working gas in a regenerator. Thus, it is necessary that a shape of regenerator be considered with the structure of heater and cooler.

(4) Rhombic mechanism

Schematic view of a Rhombic mechanism is shown in Fig. 5(a). It consists of two gears, two yokes and four connecting rods. In the figure, when length of the connecting rod, L, length of crank arm, R, and leaning distance, e, were set to a suitable ratio, phase angle between a displacer and a power piston was set to 90 degrees. In this mechanism, both pistons move in a straight line completely, if it is assembled ideally. However, when it has not sufficiently high assembling accuracy, the side thrust force and friction loss of the both pistons increase. In order to make the friction loss low enough even if the assembling accuracy was not good, several free joints were added to the power piston and to the displacer rod of the prototype engine as shown in Fig. 5 (b).

The crankcase for the Rhombic mechanism tends to become a bigger size than those of a Scotch-yoke mechanism and a general crank mechanism. Thus, whether the Rhombic mechanism is good for the engine size reduction depends on the balance of several factors. It is considered that the optimal mechanism in view of getting smaller engine is clarified based on experimental researches in the next step.

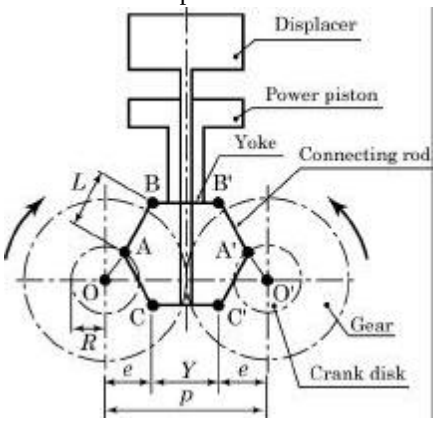

(a) Outline of Rhombic mechanism

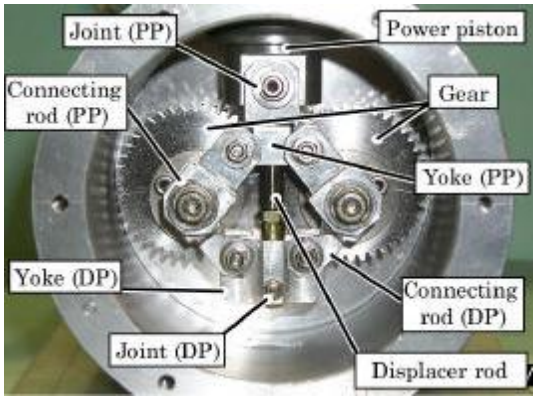

(b) Rhombic mechanism of the prototype engine

Fig. 5 Rhombic mechanism

(5) Seal device

As seal devices of the prototype engine, there were piston rings of the displacer and the power piston, a reciprocating rod seal at a displacer rod, a rotating rod seal at an output shaft. The prototype engine was designed to use various types of seal devices. In the first manufacturing, a straight cut ring of 2 mm width was used as the piston ring of the displacer. An endless ring of 19 mm width was used as the piston ring of the power piston. Because, the endless ring has higher seal performance than that of a straight cut ring. It also works as a linear guide for a straight motion of the power piston. A linear bearing was used as the reciprocating rod seal at the displacer rod. In the following experiment to measure mechanical loss, a lip seal was used as the rotating rod seal at the output shaft. All of the above seal devices were made of PTFE.

3. ENGINE PERFORMANCE

The prototype engine was manufactured as shown in Fig. 6. At the first trial of operation, the prototype engine did not work well under pressurized condition. Thus, in order to investigate the causes, the prototype engine was experimented in detail as follows.

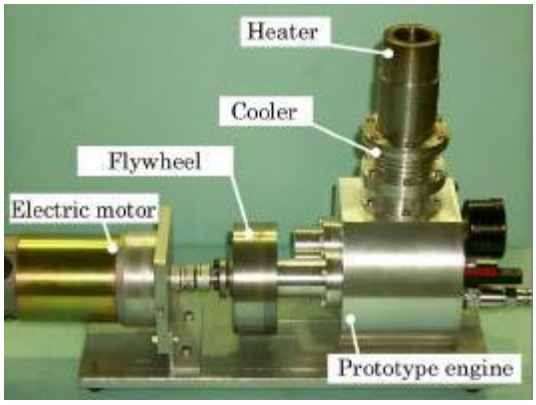

Fig. 6 Prototype Stirling engine

3.1 EXPERIMENTAL RESULTS USING AIR IN ATMOSPHERIC CONDITION

The prototype engine was experimented using air in atmospheric condition and no load condition. In the experiment, an electric heater was used as heat source, and heat input, Qin, was changed from 200 to 500 W in steps. The prototype engine was cooled by the water running the cooler jacket. The flow rate of cooling water was 1.7 L/min constantly. Measuring points of gas pressure and temperature are shown in Fig. 3. Expansion space gas temperature, T_E, compression space gas temperature, T_C, and heater all temperature, T_w was measured by thermocouples.

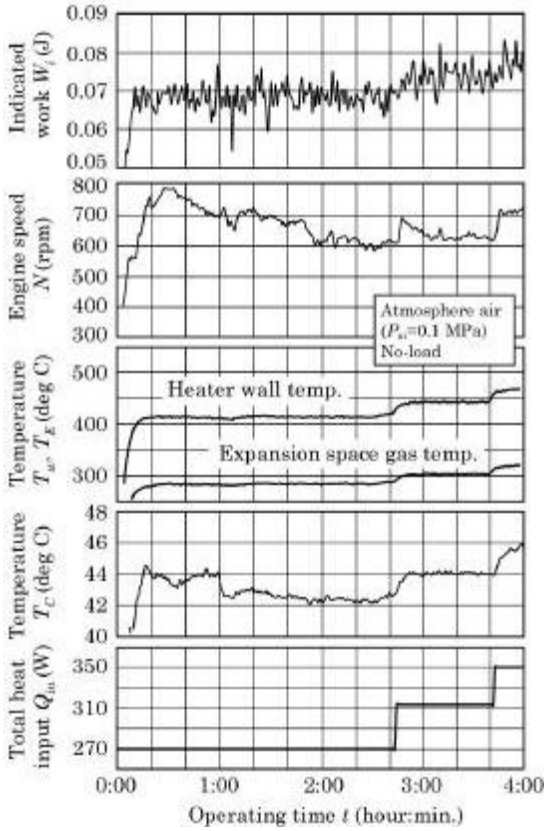

Fig. 7 Experimental results as a function of operating time

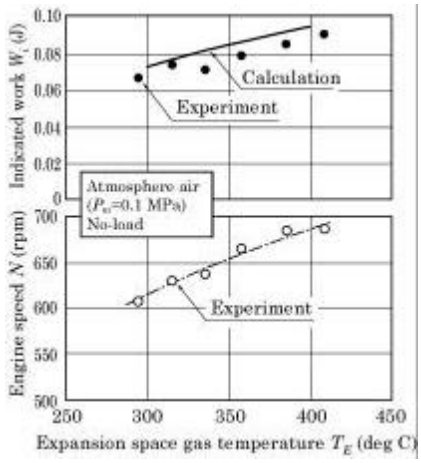

Fig. 8 Engine Speed and indicated work as a function of expansion space gas temperature

Figure 7 shows the experimental results of heat input, Qin, eater wall temperature, T_w, expansion space gas temperature, T_E, compression space gas temperature, T_C, engine speed, N, and indicated work, W_i, with operating time, t; t=0 corresponds to the start of heating. In the figure, it is shown that the engine starts to run just after the start of heating, and engine speed increases to about 00 rpm after 30 minutes. Then, engine speed decreases slowly, and keeps about 600 rpm after 1.5 hours. After then, engine speed increases with increasing heat input,

Qin, temporally. However, it decreases with time. The power in this operating condition is smaller than that of rated operation. Therefore, it is considered that the effects of friction loss in mechanical devices and gas leakage from the power piston were relatively bigger. Figure 8 shows the relationship between expansion space gas temperature, T_E, engine speed, N, and indicated work, Wi, at a steady state. The calculated result of indicated work, Wi, was derided from an isothermal analysis [4] with considerations of pressure loss in the regenerator and gas leakage from the power piston. Calculated conditions were based on the experimental results approximately. In the case of the experiment, engine speed, N, and indicated work, W_i, increased with increasing of expansion space gas temperature, T_E.

The calculated result of indicated work, W_i, is similar to that of the experimental result comparatively, though the calculated result is about 7 % lower than the experimental result. Thus, it is confirmed that the prototype engine works correctly under atmospheric condition.

3.2 MEASUREMENT OF MECHANICAL LOSS

In order to measure mechanical loss, the prototype engine was driven by an electric motor as shown in Fig. 6. Mechanical loss, L_m, and friction torque, T_{qm}(=60L_m/2N), were derived from driving torque of the electric motor and indicated work of the engine. In this experiment, the lip seal was set at the output shaft, and working space and buffer space (behind the power piston) were pressurized to 1 MPa maximum with nitrogen. The prototype engine was not heated in this experiment, and working space temperature kept room temperature approximately. Figure 9 shows the relationship between angular speed, w(=2N/60), and friction torque, T_{qm}. In the figure, friction torque, T_{qm}, increases with increasing of angular speed, w, linearly. In a research by the author [4], it was confirmed that if mechanical loss consisted of the Coulomb friction loss that depends on vertical force and the viscosity friction loss that depends on speed, viscosity coefficient, then c_v, was equivalent to an inclination of this line. The inclination was constant at various pressure, and viscosity coefficient, c_{vi}, was determined to be 2.03´10-4(Nms) from Fig. 9. on the other hand, in the range of higher engine speed, such as N>2000 rpm, a noise was generated periodically from a hot side of the cylinder. It was caused by a collision between the displacer and the cylinder, because the Rhombic mechanism of this engine did not have high assembling accuracy.

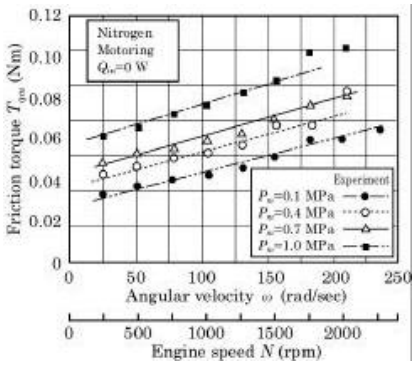

Fig. 9 Experimental result of friction torque

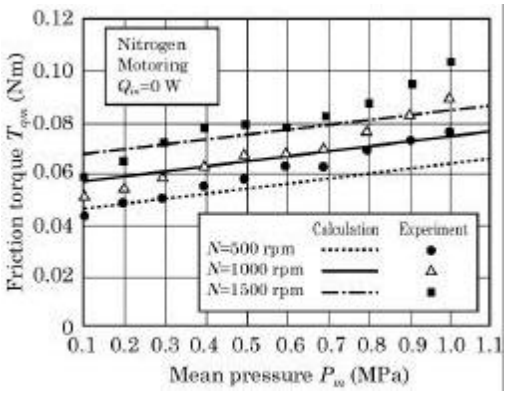

Fig. 10 Friction torque as a function of mean pressure

Figure 10 shows the experimental and calculated results of the relationship between mean pressure, Pm, and friction torque, T_{qm}. The calculated result was gotten using the Coulomb friction loss of each seal device and bearing, and the viscosity friction loss. The calculated result agreed with the experimental result approximately in the range of lower pressure. However, the experimental result of friction torque, T_{qm}, became larger than that of the calculated result with increasing of mean pressure, P_m. It was caused by the increasing of friction force, which derived from low assembling accuracy of the Rhombic mechanism.

3.3 COMPARISON TO SIMULATION

Based on the above experimental results, a simulation method with consideration of mechanical loss was developed. Figure 11 shows the experimental and calculated result of the relationship between engine speed, N, indicated power, L_i, shaft power, L_s, at mean pressure, Pm, of 0.8 MPa using helium as working gas. In this experiment, the prototype engine was driven by the electric motor. The electric heater was used as a heat source. Heat input of the electric heater, Q_{in}, maintained the expansion space gas temperature, T_E, at 450° C. In the figure, the experimental result of indicated power is about 25 % lower than that of the calculated result. The expansion space of the prototype engine is divided into the inside space and the outside space by the heater inner tube as shown in Fig. 3. Thus, expansion space gas temperature is not necessarily uniform. It is considered that expansion space gas temperature in the inside space becomes fairly lower than that of measured temperature, TE. Therefore, in order to unify the expansion space gas temperature and get higher power of the engine, a development of a high performance heater and discussion of a heating method are needed in the next step. On the other hand, in this experiment, compression space gas temperature, T_C, reached about 60° C. In order to get lower compression space gas temperature and higher power of the engine, a development of a high performance cooling system is needed.

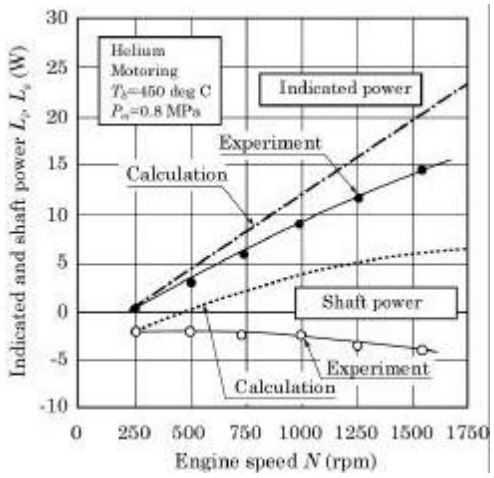

Fig. 11 Power as a function of engine speed

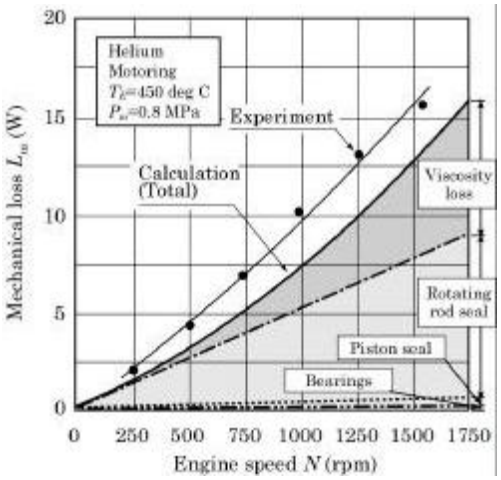

Fig. 12 Mechanical loss as a function of engine speed

Figure 12 shows the experimental and calculated results of the relationship between engine speed, N, and mechanical loss, Lm. The tendency of the calculated result agrees with that of the experimental result approximately, though the calculated result is 20~25 % lower than that of the experimental result. With regard to the detail of calculated mechanical loss, friction loss of piston seals and bearings was very small, and it was about 5~6 % of the Coulomb friction loss. On the other hand, friction loss of the rotating rod seal at the output shaft reached to about 94 % of the Coulomb friction loss.

4. DISCUSSIONS FOR HIGH PERFORMANCE

In this paper, the compact Stirling engine that has unique components is introduced. It is considered that there are many effective results from the analysis methods to the components' design. However, the performance of the prototype engine was far from the target performance. In this chapter, methods for improvement of performance are suggested as follows.

4.1 HEAT EXCHANGERS

A simple moving-tube-type heat exchanger was designed and manufactured. However, it was not high performance in focus of heat transfer. It will be improved if the gas temperature in expansion space is close to uniform, as described above. Thus, the author has developed several types of the heater as shown in Fig. 13. Type A is the same as that of Figs. 2 and 3. Type B has simpler structure, still more; it is expected to unify the expansion space gas temperature. However, there is a strong possibility that heating surface area decreases if the size of the heater is the same as Type A. As the next step, it is necessary to analyze heat transfer performance of the moving-tube-type heat exchanger in detail.

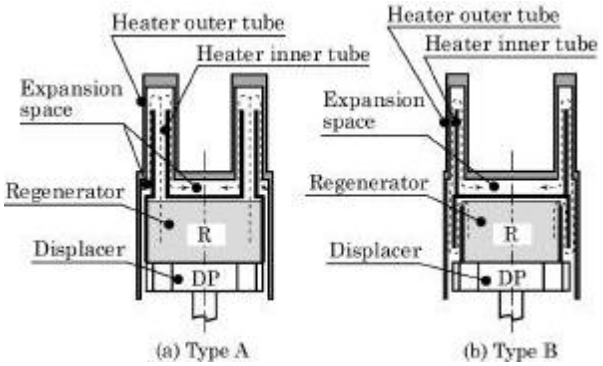

Fig. 13 Improvement of moving-tube type heat exchanger

4.2 PISTON DRIVE MECHANISMS

As a piston drive mechanism, the Rhombic mechanism was adopted for the prototype engine. It has several the free joints that are located at the power piston and the displacer rod as shown in Fig. 5 (b). It was confirmed that the mechanism with free joints worked correctly. However, in order to decrease mechanical loss, and to make the piston movement more close to the straight movement, it is necessary that the mechanism have higher assembling accuracy.

Under the above considerations, the Rhombic mechanism has been improved. For an example, Figure 14 shows the mechanical parts with an additional free joint for the power piston.

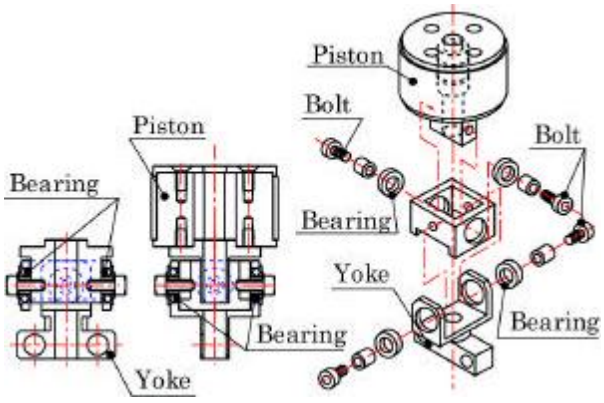

Fig. 14 Improved piston drive mechanism

Also, this paper does not discuss manufacturing accuracy and endurance of the piston drive mechanism. A detail analysis related to mechanical loss and an endurance test is needed in the next step.

4.3 HERMETIC GENERATOR SET

The rotating rod seal at the output shaft has large mechanical loss as described above (see Fig. 10). The seal can be omitted, if the electric generator is put in the pressurized crankcase, because the shaft does not penetrate the crankcase in that case. It is considered that the mechanical loss decreases remarkably, and the shaft

power increases fairly with the hermetic generator set. Figure 15 shows the developed hermetic generator set.

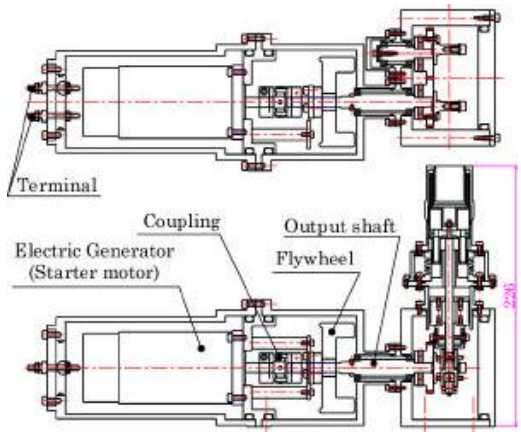

(a) Schematic view of the hermetic generator set

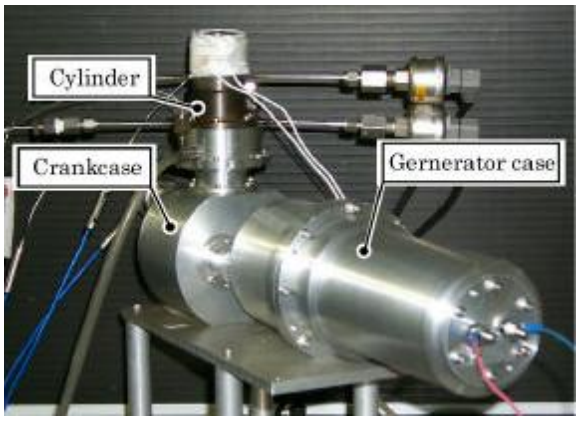

(b) The hermetic generator set on a test bench

Fig. 15 Hermetic generator set condition

However, the measurement of the characteristics of the generator set was not done yet. Also, the electric generator shown in Fig. 15 had big size, because it needed enough capacity for the experiments at wide-range speed condition. It can realize a more compact size generator set, if the engine works only at rated operation in practical use.

5. CONCLUSION

In this paper, a prototype Stirling engine was developed with purposes to get a compact and low cost Stirling engine. The prototype engine was experimented using air in atmospheric condition and with no load. Also, mechanical loss under pressurized condition was measured. It was discussed how to get higher performance based on the experimental and calculated results. As the results, it was confirmed that the development of higher performance heat exchangers and decreasing of mechanical loss were required. On the other hand, it was considered that a compact Stirling engine was optimized by detailed measurements for a heat balance. As the next step, the author aims to get the target power, 50 W, and will investigate the detail of heat balance. This research aimed at the development of a compact Stirling engine with low production cost. When the compact, low cost and high performance Stirling engine is developed, it will contribute to solution of environmental pollution and energy utilization.

REFERENCES

[1] Iwamoto, S., Hirata, K. and Toda, F., " Performance of Stirling Engines (Arrangement for Experimental Results and Performance Prediction Method) (in Japanese)", Transactions of the Japan Society of Mechanical Engineers, No. 65, Vol. 635, B, p. 361-368 (1999).

[2] Endo, N., Hasegawa, Y., Shinoyama, E., Tanaka, A., Tanaka, M., Yamada, Y., Takahashi, S. and Yamashita, I., "Test and Evaluation Method of the Kinematic Stirling Engines and Their Application Systems Used in the Moon Light Project", Proc. of 4th International Conference on Stirling Engines, p. 315-320 (1988).

[3] Hirata, K., Kagawa, N., Yamashita, I. and Iwamoto, S., "Basic Study on Development of Stirling Engine for Small Portable Generator (1st Report, Engine Design, Manufacturing, and Performance) (in Japanese)", Transactions of the Japan Society of Mechanical Engineers, Vol. 64, No. 621, B, p. 1600-1607 (1998).

[4] Hirata, K., Hamaguchi, K. and Iwamoto, S., "Basic Study on Development of Stirling Engine for Small Portable Generator (2nd Report, Engine Performance Prediction by Simulation Model) (in Japanese)", Transactions of the Japan Society of Mechanical Engineers, Vo. 64, No. 621, B, p. 1608-1615 (1998).

[5] Hargreaves, G. M., "The Philips Stirling Engine", p. 130-141 (1991), Elsevier.

[6] Yamashita, I., Hamaguchi, K., Kagawa, N., Hirata, K. and Momose, Y., "Theory and Design of Stirling Engines (in Japanese)", (1999), Sankaido.

[7] Fawad Ahmeda, Huang Hulin. Numerical modeling and optimization of beta-type Stirling engine[J]. Applied Thermal Engineering, 2019, 149: 385–400

[8] Metin Güven , Hasan Bedir. Optimization and application of Stirling engine for waste heat recovery from[J]. Energy Conversion and Management, 2019, 180 :411–424

[9] Halit Karabulut, Melih Okur. Performance prediction of a Martini type of Stirling engine[J]. Energy Conversion and Management, 2019, 179:1–12

[10] S.A. El-Ghafour, M. El-Ghandour. Three-dimensional computational fluid dynamics simulation of stirling[J]. Energy Conversion and Management, 2019, 180:533–549

[11] Halit Karabulut, Melih Okur. Thermodynamic, dynamic and flow friction analysis of a Stirling engine with Scotch yoke piston driving mechanism[J]. Energy, 2019, 168 169-181

[12] Oscar R. Sandovala, Bryan Castro Caetano. Modelling, simulation and thermal analysis of a solar dish Stirling system A case study in Natal, Brazil[J]. Energy Conversion and Management, 2019, 181 189–201